ASSESSMENT OF ALPHAMAGNETIC SPECTROMETER (AMS) UPPER EXPERIMENT STRUCTURAL CONFIGURATION SHIELDING EFFECTIVENESS ASSOCIATED WITH CHANGE FROM CRYO-COOLED MAGNET TO PERMANENT MAGNET

Robert Scully [1]

[1] *NASA, 2101 NASA Parkway, Mail Stop EV511, Houston, TX, 77573, US, Email: robert.c.scully@nasa.gov*

ABSTRACT

In the spring of 2010, the Alpha Magnetic Spectrometer 2 (AMS-02) underwent a series of system level electromagnetic interference control measurements, followed by thermal vacuum testing. Shortly after completion of the thermal vacuum testing, the project decided to remove the cryogenically cooled superconducting magnet, and replace it with the original permanent magnet design employed in the earlier AMS-01 assembly. Doing so necessitated several structural changes, as well as removal or modification of numerous electronic and thermal control devices and systems. At this stage, the project was rapidly approaching key milestone dates for hardware completion and delivery for launch, and had little time for additional testing or assessment of any impact to the electromagnetic signature of the AMS-02. Therefore, an analytical assessment of the radiated emissions behavioural changes associated with the system changes was requested.

1. GENERAL DESCRIPTION OF THE AMS-02

The AMS-02 is a state-of-the-art particle physics detector designed, constructed, tested, and operated by an international team organized under United States Department of Energy (DOE) sponsorship. The science objectives of the AMS are to search for antimatter, dark matter, and to understand cosmic ray propagation and confinement time in the galaxy.

The AMS-02, shown in Fig. 1, utilizes a large permanent magnet to produce a strong, uniform magnetic field over a large volume. The magnetic field is used to bend the path of charged cosmic particles as they pass through five different types of detectors. The Transition Radiation Detector (TRD) is used to distinguish between particles having low mass, such as electrons and positrons, and particles having comparably great mass, such as protons and anti-protons. The Time of Flight (TOF) detector measures the charge and velocity of passing particles, and their transit time as they pass through the magnetic field. Silicon Tracker detectors measure the coordinates of charged particles as they pass through the magnetic field, and are the only detectors able to distinguish directly between matter and antimatter. Matter and antimatter will bend in opposite directions, and the

radius of curvature of the path the particle follows can be used to estimate the particle's momentum.

Figure 1. Image of the AMS-02

The Ring Image Cerenkov Counter (RICH) measures the velocity of particles, which data is used in the determination of particle mass. The Electromagnetic Calorimeter (ECAL) measures the energy and coordinates of electrons, positrons and gamma rays, and allows the AMS-02 to distinguish protons from positrons, and electrons from anti-protons. Fig. 2 shows the AMS-02 detector and its response to different particles or nuclei. With over 300,000 data channels, the detector gathers an extremely large amount of data which is then processed and sent to Earth utilizing the International Space Station (ISS) power, communication and data infrastructure.
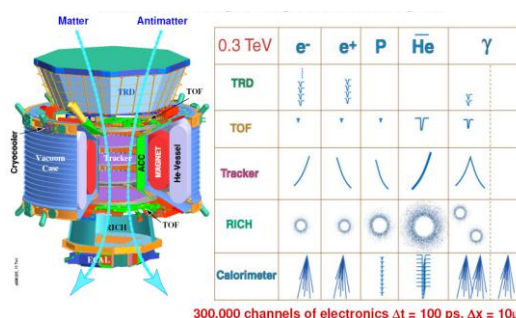

Figure 2. AMS-02 Experiment Response Signatures

The AMS-02 also has an Anti-Coincidence Counter, used to reject signals associated with cosmic rays and particles that do not traverse the experiment from top to bottom, a Tracker Alignment System, used to

periodically check and correct for any misalignment of the Silicon Tracker planes, two star trackers, and a GPS system.

2. BACKGROUND

In the spring of 2010, the AMS-02 was undergoing its final certification testing. Electromagnetic interference control testing was performed in the late February, early March time frame. As part of the testing procedures, the radiated emissions (RE) of the AMS-02 were measured using standard procedures as detailed in the International Space Station documents SSP30237, Space Station Electromagnetic Emission and Susceptibility Requirements, and SSP30238, Space Station Electromagnetic Techniques. Emissions were collected in 4 different positions surrounding the AMS-02 structural configuration, typically represented by the photos shown in Figs. 3 and 4. MultiLayer Insulation (MLI) blankets were in place surrounding the Transition Radiation Detector (TRD), and the zenith radiator structure was in place above the TRD MLI covering.

During testing, the payload was powered up in its nominal start-up mode. All systems / sub-systems were powered on through nominal AMS-02 detailed test procedures, and remained powered for each test.
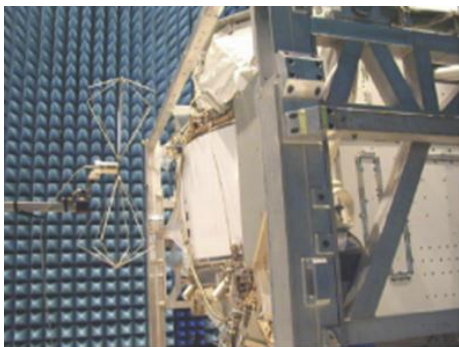

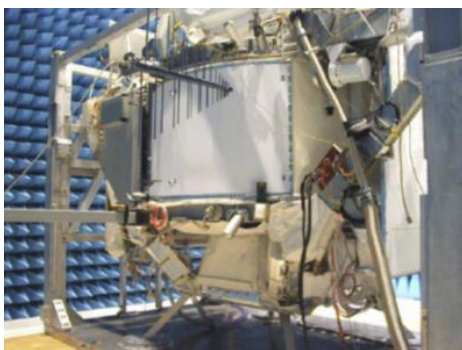*Figure 3. Relative Measurement Position #1*

Figure 4. Relative Measurement Position #4

The AMS-02 was compliant with the SSP30237 radiated emissions requirement RE02 except for some observed non-compliances between 7 MHz and just above 10 MHz, and between 259 MHz and just above 1.1 GHz. Fig. 5 illustrates typical observed performance.
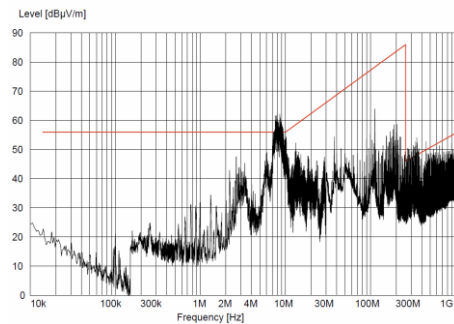

Figure 5. AMS-02 RE Performance in Nominal Configuration

Following the electromagnetic interference control testing, thermal vacuum testing was performed. Shortly after completion of the thermal vacuum testing, the AMS-02 project made a decision to replace the superconducting magnet with the AMS-01 permanent magnet. The permanent magnet presented the opportunity to gather science for a longer duration than obtainable with the superconducting magnet. In addition, the superconducting magnet presented additional risks that the AMS-02 project ultimately chose not to accept.

3. ELECTRICAL AND MECHANICAL CHANGES PERTINENT TO SHIELDING EFFECTIVENESS OF THE UPPER STRUCTURE OF THE EXPERIMENT

Removal of the superconducting magnet entailed a large number of mechanical and electrical changes. All of the cryogenic system components were removed, as well as all of the electrical and electronic components associated with the operation and control of the cryogenic system. Fig. 6 highlights the removal of many potential sources of electromagnetic interference that were removed from the AMS configuration previously tested, including cryomagnet avionics, baroswitch electronics, the cryomagnet pilot valve switch, the uninterruptible power supply, the vent pump and its cabling, and cabling associated with cryogenic charging and discharging functions.

Commensurate with the removal of the cryogenic system, several additions were required to accommodate the magnet change, including the installation of the permanent magnet, new mechanical support structures, new silicon tracker planes, new heaters, new thermal blankets to cover the upper structure, new light blocking and containment materials for tracker planes 1N and 6, and new Tracker plane cabling.
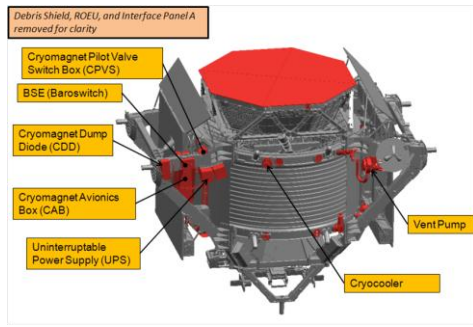
Figure 6. Schematic Diagram Illustrating Removed Electrical and Electronic Components

Figs. 7 and 8 highlight the primary regions of change in the AMS-02 structure most expected to affect the radiated emissions signature. Several changes occurred in the topmost section of the experiment, driven by thermal considerations. The changes that most directly impact the shielding effectiveness of the upper portion of the experiment structure are the removal of the zenith radiator, the relocation of the tracker plane and its associated support structure, and the extension of the MLI to enclose the newly configured upper structure.
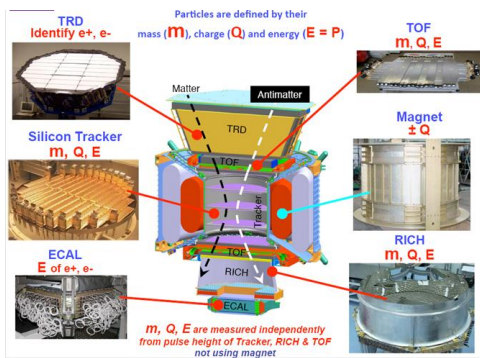

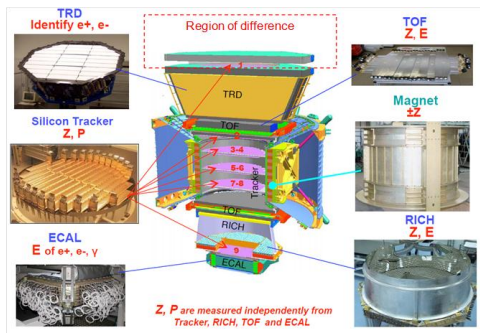*Figure 7. AMS-02 Configuration w/ Cryogenic System*

Figure 8. AMS-02 Configuration w/o Cryogenic System

4. ASPECTS OF SHIELDING EFFECTIVENESS OF THE BASELINE CONFIGURATION

Starting from the TRD cover and working upwards, the shielding effectiveness of the baseline structure is based

on that of the TRD cover itself, the MLI over the TRD cover, and the zenith radiator, mounted above the MLI over the TRD cover.

The TRD cover is fabricated of a honeycomb aluminum core comprising hex cells 90.6 mm in length, each with a diameter of 4.76 mm, and each having 0.032 mm walls, sandwiched between carbon fiber composite (CFC) sheets top and bottom. The CFC sheets are each 0.50 mm thick. Using standard shielding equations for the CFC sheets and the honeycomb material yields theoretical attenuation values as shown in Fig. 9.
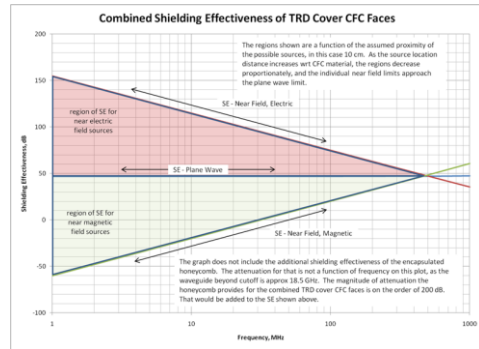

Figure 9. Theoretical Attenuation Factors for the TRD CFC Sheets and Enclosed Honeycomb Material

The MLI comprises standard materials as used in many different NASA applications. Stack-ups of the layers for the TRD blankets are shown in Tab. 1. Measurements of the MLI thickness were made at the center of the blanket, at a typical seam, and at a finished edge.

Table 1
AMS-02 Blankets Used on Sides and Top of TRD Structure

Materials	# Layers
AMS02 blanket layup, TRD_Top	
aluminum/reinforced Kapton	1
double-sided PET/ aluminum & scrim	10
aluminum/reinforced Kapton	1
AMS02 blanket layup, TRD_Edge	
800 DUN_MET aluminum/Beta cloth	1
double-sided PET/ aluminum & scrim	10
aluminum/reinforced Kapton	1
AMS02 blanket layup, TRD_Side	
800 DUN_MET aluminum/Beta cloth	1
double-sided PET/ aluminum & scrim	7
aluminum/reinforced Kapton	1

Uncompressed thicknesses ranged from 1.0 mm for the center of the blanket, 1.5 mm for the seam, and 2.0 mm for the finished edge. Photos of the TRD MLI configuration are shown in Figs. 10 and 11.
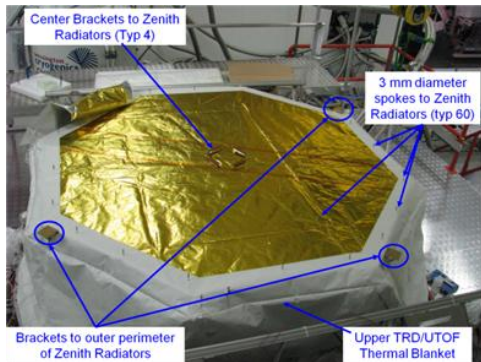

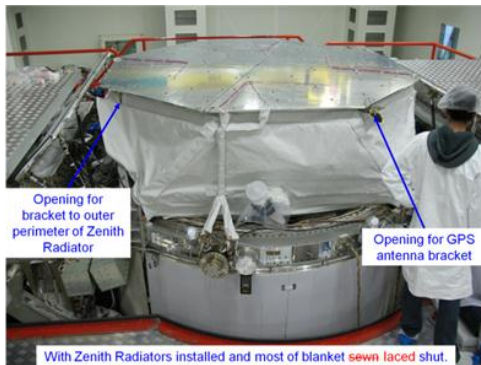*Figure 10. MLI in Place Over TRD Structure*

Figure 11. Nearing Completion of MLI Installation, Showing Zenith Radiator in Place

All MLI layers in each blanket are electrically bonded to each other and to the AMS-02 structure using a stack-up of washers on a threaded fastener, wherein the washers are located interstitially between MLI layers. The washers and MLI layers are compressed by a nut on the threaded fastener, and an electrical bonding wire lead is captured under the head of the fastener and held in place with Kapton tape against the inner surface of the MLI. Fig. 12 illustrates this stack-up of fastener, washers, and MLI layers.
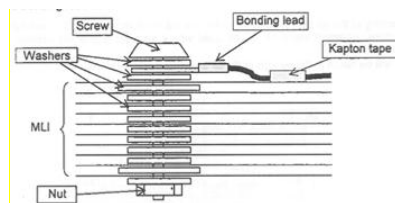

Figure 12. Electrical Bonding Stack-Up for MLI

Given the MLI layers are well bonded electrically as described in Fig. 12, and the construction and metallization of the layers of the MLI as described in Tab. 1, it is reasonable to expect that the MLI will perform well as a shield that is electrically continuous with the structure itself. Shielding effectiveness for the blankets is a function of the ability of the aluminum metallization on each of the various layers to provide a barrier. While it is attractive to assume that the total shielding is the sum of the shielding afforded by all the layers added together, various aspects of blanket use including cracking and degradation with installation, removal, thermal effects, aging, and so forth drive to a conservative estimate for the total shielding being equal to that of a single layer. Again using standard equations for shielding effectiveness, the theoretical attenuation for a single layer of MLI is shown in Fig. 13.
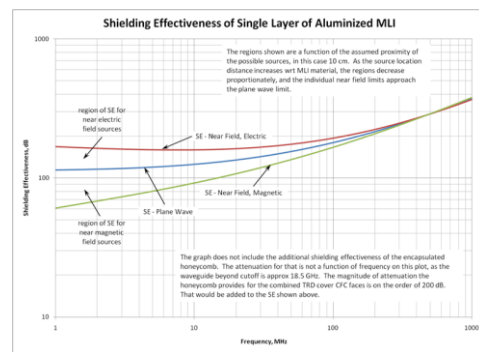

Figure 13. Theoretical Shielding Effectiveness for a Single Layer of MLI

The MLI over the TRD cover does have a number of intentional openings, and these openings will act to reduce the shielding effectiveness of the blanket to some degree. Approximately 60 penetrations through the MLI are made to accommodate the zenith radiator support spokes. Additional openings exist for support/mounting brackets for the zenith radiator, 4 in the center for the zeta brackets, and 4 more openings for the stiff brackets spaced symmetrically at the edge of the TRD, and an opening to allow passage of an RF cable and to accommodate the mounting bracket for a GPS antenna. The holes in the MLI would act to reduce the shielding effectiveness by no more than 20 dB from the magnitude associated with an unadulterated MLI.

The zenith radiator assembly comprises 4 separate plates, one each for the 4 separate cryo-cooling systems on-board the AMS-02. A photograph of the zenith radiators installed on top of the AMS-02 structure is shown in Fig. 14. From Fig. 14, it is clear that a gap does exist between each of the 4 radiator panels, estimated on the order of 6 to 10 mm. Each panel comprises a top and sheet of aluminum, 1.6 mm thick, a core of Rohacell dielectric material, and a bottom sheet of aluminum, 0.3 mm thick. The panels also have cryo-coolant tubing, and a number of inserts to accommodate the support spokes, mounting fasteners, and attachment

of 3 electrical bonding straps per panel to join the top and bottom aluminum sheets together.
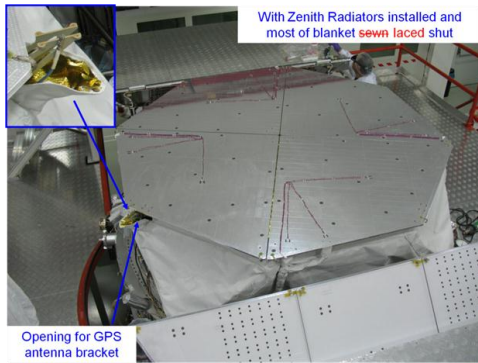

Figure 14. Photograph of Installed Zenith Radiators and Highlight of GPS Antenna Opening in MLI

Some of the electrical bonding straps are visible in Fig. 14, near the apexes of the two panels shown in the lower portion of the photograph. Additional electrical bonding straps, 1 per panel, not visible in Fig. 14, are used to electrically connect the panels to the TRD structure. From an electrical shielding perspective, the interior mechanical components of the panels are of no consequence. Only the top and bottom sheets of aluminum, and the electrical continuity of the two sheets to the TRD structure is of any importance. The aluminum sheets will provide excellent shielding by themselves, but this is negated to a large extent by the 6 to 10 mm gap between each of the four panels, and the vertical separation on the order of 60 mm between the upper surface of the MLI TRD cover and the lower panel surfaces.

A review of the theoretical shielding effectiveness of the upper experiment shows that the TRD cover and the MLI together provide substantial electromagnetic shielding to any emissions that might originate from within the TRD or the lower internal workings of the AMS-02 magnet assembly, leading to the conclusion that the typically observed radiated emissions such as those shown in Fig. 5 were primarily the result of emissions associated with electrical and electronic components and subsystems, and their associated cabling, mounted external to the magnet assembly.

5. DISCUSSION OF MODIFEID CONFIGURATION

In the modified configuration, all of the components associated with the cryo-cooling systems associated with the cryomagnet were removed, as previously discussed, thereby substantially reducing the number of electrical and electronic noise sources on the AMS-02 structure.

The upper TRD CFC was covered with a 0.05 mm layer of aluminum foil, as shown in Fig. 15. The TRD otherwise remained the same physically. The addition of the layer of aluminum foil would dramatically improve the shielding effectiveness of the TRD upper cover, with an expected performance much like that of a single layer of aluminized MLI.
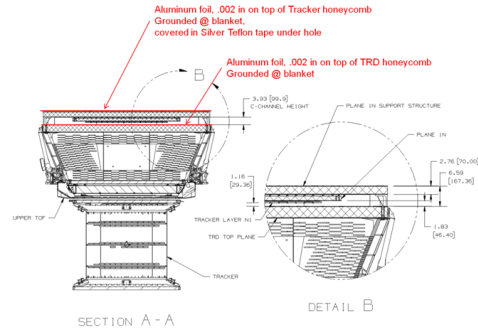

Figure 15. Highlight of AMS-02 Structure, Indicating Addition of Aluminum Foil to TRD Upper Cover and Top of the Relocated Tracker Plane

The tracker plane 1N was relocated to the top of the TRD structure. The plane and its support structure, shown in Fig. 16, comprises the tracker layer, the tracker plane, the tracker plane support structure, a carbon containment channel, and a 0.05 mm thick layer of aluminum on top of the tracker support structure. The tracker layer faces the TRD cover.
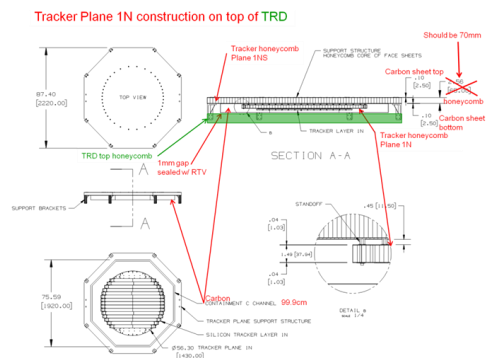

Figure 16. Tracker Plane 1N Structure/Installation

The overall shielding effectiveness of the assembly is dominated by the combined performance of the CFC honeycomb structure, expected to be entirely analogous with the performance of the TRD cover, and the aluminum foil covering the upper surface of the tracker support layer. As already stated, the aluminum foil is expected to demonstrate similar performance to that of a single layer of aluminized MLI.

Finally, the entire added assembly of the tracker layer, the tracker plane, and the tracker support structure, is completely surrounded and covered by a continuous

layer of MLI, extended from the previous MLI covering the TRD structure, expected to exhibit entirely similar shielding performance as already shown for a single layer of aluminized MLI. The sole difference on the MLI covering as compared to that of the original design is the presence of a 40 cm by 40 cm opening in the center of the MLI above the tracker support structure. This opening itself is covered by a type 316 stainless steel mesh having 50 openings per 2.54 cm, with an overall thickness of 0.061 mm. The wire diameter is 0.0305 mm. The shielding effectiveness of this mesh from the vendor, TWP Inc, is shown in Fig. 17.
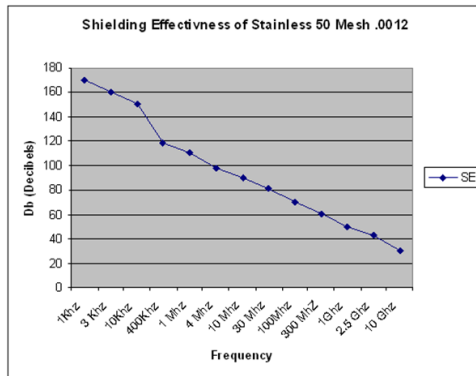

Figure 17. Shielding Effectiveness of 50 Mesh T3316 Stainless Hi Transparency

So, the opening will allow a leakage of RF from the interior of the MLI shroud, but with the very high shielding effectiveness of the tracker support structure, the tracker plane, the tracker layer, and the TRD cover, the leakage amount should be negligible.

6. EXPECTED IMPACT TO RE02 MEASUREMENTS

Review of the theoretical shielding effectiveness contributions of the various components of the original configuration strongly suggest that the radiated emissions performance as observed in the certification measurements was almost certainly the result of emissions from the equipment mounted to the exterior of the magnet housing, and not from any disturbances originating from within. With the removal of the cryomagnet and relocation of the tracker 1N layer to above the TRD upper cover, together with the addition of the MLI shrouding the new structure, it is very likely that the shielding effectiveness of the modified configuration is at least as good as the original configuration, if not actually improved.

Further, the removal of the several electrical and electronic systems from the exterior of the magnet housing should act directly to reduce the spectral content of measurable radiated emissions for the AMS-02 assembly, were such measurements to be repeated.

Moreover, it is extremely unlikely that any new frequencies would appear in the spectral content, since no new electrical or electronic equipment was introduced concomitant with the magnet changeout.

7. CONCLUSION

Based on the above examination and review, it was recommended that no further RE02 testing be performed, and that the AMS-02 permanent magnet configuration be accepted for the purposes of RE02 certification, and for safety of flight considerations.